Comparison of Denoising Algorithms for Demosacing Low Lighting Images using CFA 2.0

Chiman Kwan and Jude Larkin

Applied Research, LLC, Rockville, Maryland, USA

Abstract

In modern digital cameras, the Bayer color filter array (CFA) has been widely used. It is also widely known as CFA 1.0. However, Bayer pattern is inferior to the red-green-blue-white (RGBW) pattern, which is also known as CFA 2.0, in low lighting conditions in which Poisson noise is present. It is well known that demosaicing algorithms cannot effectively deal with Poisson noise and additional denoising is needed in order to improve the image quality. In this paper, we propose to evaluate various conventional and deep learning based denoising algorithms for CFA 2.0 in low lighting conditions. We will also investigate the impact of the location of denoising, which refers to whether the denoising is done before or after a critical step of demosaicing. Extensive experiments show that some denoising algorithms can indeed improve the image quality in low lighting conditions. We also noticed that the location of denoising plays an important role in the overall demosaicing performance.

Keywords

Bayer pattern, RGBW pattern, CFA 1.0, CFA 2.0, color filter array, demosaicing, denoising, pansharpening, deep learning

1. Introduction

Bayer pattern [1] was invented in the early 1980's and is still a very popular color filter array (CFA) for digital cameras. The Bayer pattern as shown in Figure 1(a) is also known as CFA 1.0 in the literature. Even for planetary explorations, NASA has adopted the Bayer pattern in the Mastcam imagers onboard the Mars rover Curiosity [2]-[5].
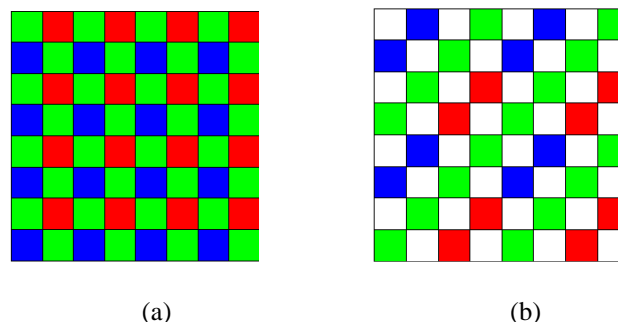
(a)   (b)

Figure 1. Two CFA patterns. (a) CFA 1.0; (b) CFA 2.0.

Aiming to improve the Bayer pattern in low lighting conditions, Kodak researchers [6,7] invented a red-green-blue-white (RGBW) CFA pattern, which is also known as CFA 2.0, as shown in

Figure 1(b). Half of the pixels in CFA 2.0 are white and the remaining pixels share the R, G, and B colors. Due to the presence of white pixels, the camera sensitivity is increased and hence the performance of CFA 2.0 in low lighting conditions should be better than CFA 1.0. Extensive experiments in [8] showed that CFA 2.0 is in indeed better than CFA 1.0 in low lighting conditions, where Poisson noise is dominant. Figure 2 shows a clean color image and two noisy images with different levels of Poisson noise. It can be seen that the noise can seriously affect the visual quality of the images. In low lighting conditions, demosaicing methods alone are not sufficient in suppressing the noise. Although there are some joint demosaicing and denoising algorithms such as [9] in the literature, those algorithms are tailored to only Gaussian noise. In an earlier paper [8], we developed new demosaicing algorithms for CFA 2.0. In the process, we also investigated the impact of denoising on the overall image quality. However, the denoising investigation in [8] was limited to only one method, the block matching in 3D (BM3D), even though the performance BM3D is reasonable.
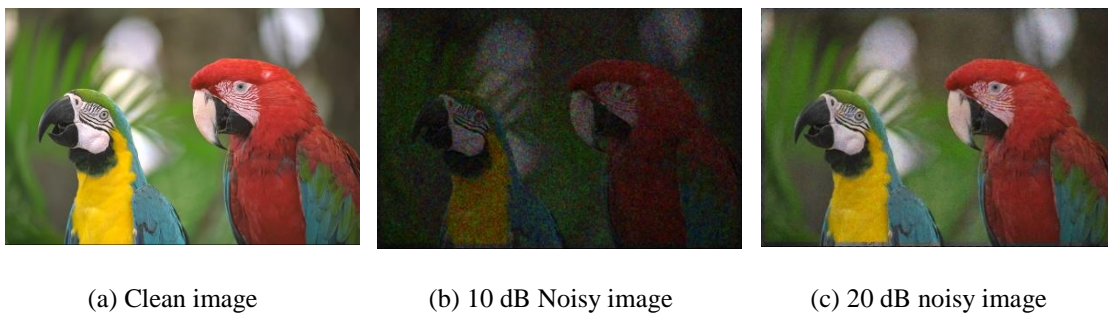

| (a) Clean image | (b) 10 dB Noisy image | (c) 20 dB noisy image |

Figure 2. Comparison of clean and noisy images with different levels of Poisson noise.

To the best of our knowledge, joint denoising and demosacing for CFA 2.0 is underdeveloped in the literature. In this paper, we will thoroughly investigate different algorithms in dealing with Poisson noise. We focus on CFA 2.0 because it was concluded in our earlier papers [8]10]-[12] that CFA 2.0 has better performance in low lighting conditions. Since only one denoising algorithm was used in [8], we would like to investigate how much performance we can further improve if we adopt other conventional and new denoising algorithms. In particular, we applied six conventional and one deep learning algorithms for suppressing Poisson noise. Two signal-to-noise (SNR) levels (10 dB and 20 dB) of Poisson noise were introduced into clean Kodak images. Moreover, three denoising configurations were also investigated. This is because, in our earlier paper [8], we observed that the location of denoising can have very different overall performance in the final demosaiced images.

Our contributions are as follows. First, we thoroughly compared seven denoising algorithms for low lighting images. Some filters can improve the image quality quite significantly. Second, three denoising configurations were studied. One configuration works better than others. Third, we are the first team to carry out denoising and demosaicing studies for CFA 2.0.

The rest of this paper is organized as follows. Section 2 summarizes the methods, data, and performance metrics. In Section 3, we present the denoising results for two noisy conditions. Finally, we conclude the paper with a few remarks and future directions.

2. METHODS, DATA, AND PERFORMANCE METRICS

2.1. Architecture

Figure 3 shows the architecture of the proposed joint denoising and demosaicing system. Given an RGBW or CFA 2.0 image, we apply the Linear Directional Interpolation and Nonlocal

Adaptive Thresholding (LDI-NAT) [13] algorithm to demosaic a reduced resolution CFA 1.0 image. Parallel to this activity, the same LDI-NAT is applied to panchromatic image with 50% pixels missing to generate a full resolution illuminance image. We use the term panchromatic or illuminance interchangeably to represent the intensity image in this paper. After the above two steps, a denoising procedure is performed on both the panchromatic image and the reduced resolution color image. The denoised image is then going through a pansharpening process to generate the demosaiced image. Finally, another post-filtering is performed. It should be noted that denoising can also be done simultaneously before and after pansharpening and we call this option the hybrid denoising scheme.

Based on the above brief description, we can have three denoising configurations:

- Pre-denoising: This means that denoising is done before pansharpening starts. As shown in Figure 3, there are two places for pre-denoising: one for reduced resolution color image and one for the full resolution illuminance or panchromatic band.

- Post-Denoising: Here, denoising is done after the demosaiced image is obtained.

- Hybrid Denoising: This configuration basically includes both pre-denoising and post-denoising.
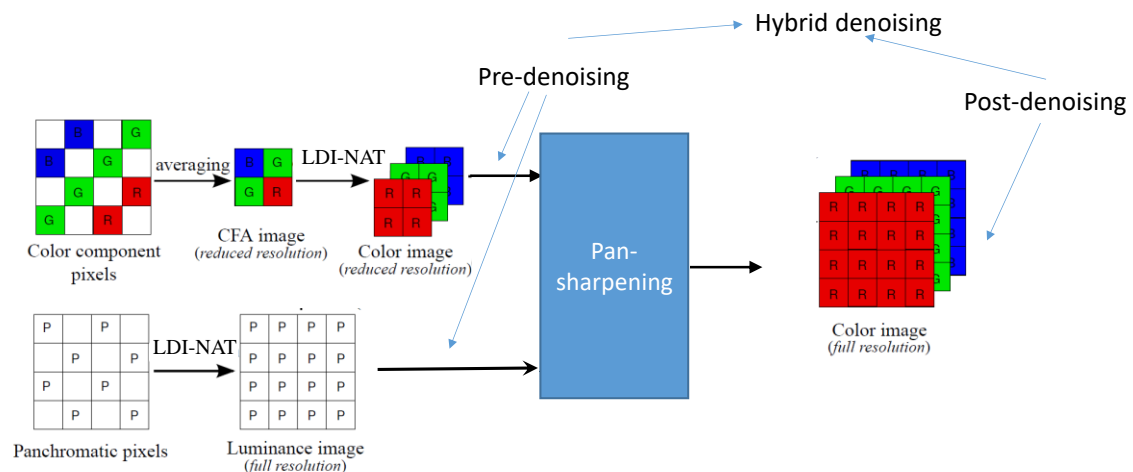

Figure 3. Architecture of joint denoising and demosaicing system for CFA 2.0.

2.2. Denoising Methods

Although there are many denoising methods in the literature, in this paper, we evaluated the following algorithms:

- Block Matching in 3 D (BM3D) [14]: This is a well-known denoising algorithm in the literature. The basic idea is to introduce exact unbiased inverses of the Anscombe and Generalized Anscombe transformations to deal with low-count (low photons) images. There are versions for Gaussian and Poisson noises. We used the version for Poisson and the codes can be found in [14].

- Wavelet [15]: The wavelet denoising consists of several steps. First, the input image is decomposed into several scales using discrete wavelet transform (DWT). Second,

thresholding is performed to the wavelet coefficients. Third, the denoising image is reconstructed from the thresholded DWT coefficients. We used the code in Matlab.

- Diffusion: According to [16], is a technique aiming at reducing image noise without removing significant parts of the image content. We used the Matlab codes [17], which does not specify whether the filter is suitable for Gaussian or other types of noise.

- Median Filter [18]: There are three variants of varying filter sizes (3x3, 5x5, 7x7). The reason for using median filters is because we observe that the noisy images have some resemblance to salt and pepper noise, which can be seen in those noisy images in Figure 2.

- FFDNet [19]: This is a deep learning based filtering algorithm. The first layer is a reversible downsampling operator which reshapes a noisy image into four downsampled sub-images. The second step involves the use of CNN for denoising. It has performed well on real images.

2.3. Demosaicing Methods

For CFA 2.0, there are not that many algorithms. In this paper, we adopted Linear Directional Interpolation and Nonlocal Adaptive Thresholding (LDI-NAT), which can be used for both demosaicing as well as interpolation [13]. It has good performance in our earlier studies [8]. We also used LDI-NAT in another earlier paper of ours [10]. As shown in Figure 3, LDI-NAT is used in two places: demosaicing the reduced resolution Bayer pattern and interpolating the panchromatic band.

In the paper [20] written by us, we proposed a pansharpening approach to demosaicing CFA 2.0. The missing pixels in the panchromatic band are interpolated. At the same time, the reduced resolution CFA is demosaiced. We then apply pansharpening to generate the full resolution color image. There are many pansharpening algorithms that can be used. Principal Component Analysis (PCA) [21], Smoothing Filter-based Intensity Modulation (SFIM) [22], Modulation Transfer Function Generalized Laplacian Pyramid (GLP) [23], MTF-GLP with High Pass Modulation (HPM) [24], Gram Schmidt (GS) [25], GS Adaptive (GSA) [26], Guided Filter PCA (GFPCA) [27], PRACS [28] and hybrid color mapping (HCM) [29]-[33] have been used in our experiments. The list is a representative, if not exhaustive, set of competitive pansharpening algorithms. Details of the above algorithms can be found in the corresponding papers and we omit the details in order to make our paper concise.

2.4. Low Lighting Images

We downloaded a benchmark data set (Kodak) from a website (http://r0k.us/graphics/kodak/) and selected 12 images, which are shown in Figure 4. It should be noted that this dataset is well-known and has been used by many authors in the demosaicing community such as [34]-[38]. These clean images will be used as reference images for objective performance metrics generation. Moreover, they will be used for generating noisy images that emulate low lighting conditions.

| Image 1 | Image 2 | Image 3 |

| Image 4 | Image 5 | Image 6 |

| Image 7 | Image 8 | Image 9 |

| Image 10 | Image 11 | Image 12 |

Figure 4. Twelve clean images from the Kodak dataset.

The process of how we introduced Poisson noise is adapted from code written by Erez Posner (https://github.com/erezposner/Shot-Noise-Generator). Details can be found in our recent paper [10]. We include the Poisson noisy 10 dB and 20 dB images in Figure 5 and Figure 6, respectively.

Image 1

Image 2

Image 3

Image 4

Image 5

Image 6

Image 7

Image 8

Image 9

Image 10

Image 11

Image 12

Figure 5. Twelve noisy images at 10 dB from the Kodak dataset.

Figure 6. Twelve noisy images at 20 dB from the Kodak dataset.

2.5. Metrics

We used the following four performance metrics to evaluate the various denoising algorithms:

- Peak Signal-to-Noise Ratio (PSNR) [39] Separate PSNRs in dBs are computed for each band. A combined PSNR is the average of the PSNRs of the individual bands. Higher PSNR values imply higher image quality.
- Human Visual System (HVS) metric Details of HVS metric in dB can be found in [40]. Higher values imply better results.

- HVSm (HVS with masking) [41] Similar to HVS, HVS incorporates the visual masking effects in computing the metrics. Higher values imply better results.
- CIELAB

We also used CIELAB [42] for assessing demosaicing and denoising performance in our experiments. Smaller values mean good results.

It should be noted that the HVS and HVSm have better correlation with human perceptions than the other three metrics [43][44].

3. EXPERIMENTAL RESULTS

In our experiments, we have used the default settings in all the denoising and pansharpening algorithms.

3.1. 10 dB Noisy Images

We first present the demosaicing results without denoising in Table 1. This will form as the baseline for comparing with those denoising results later. We observe that the averaged metrics in PSNR of all methods are all around 10 dB, meaning that demosaicing alone cannot enhance the image quality.

Table 1. Demosaicing results without denoising for 10 dB Poisson noisy images.

Image		Baseline	Standard	GSA	HCM	SFIM	PCA	GFPCA	GLP	HPM	GS	PRACS	LSLCD	Best Score
Img 1	PSNR	9.767	9.730	9.736	9.721	9.722	9.655	9.761	9.728	9.721	9.653	9.764	9.643	9.767
	Cielab	32.993	34.038	33.719	34.006	33.709	33.335	30.969	33.852	33.710	33.352	33.167	35.927	30.969
	HVS	4.162	4.151	4.152	4.142	4.151	4.070	4.172	4.146	4.147	4.082	4.162	3.891	4.172
	HVSm	4.184	4.178	4.180	4.173	4.182	4.095	4.189	4.176	4.179	4.107	4.186	3.914	4.189
Img 2	PSNR	10.283	10.294	10.294	10.290	10.299	10.223	10.298	10.295	10.301	10.228	10.301	10.321	10.321
	Cielab	23.245	23.558	23.522	23.644	23.478	23.293	22.080	23.571	23.479	23.262	23.431	24.207	22.080
	HVS	5.584	5.598	5.597	5.597	5.605	5.516	5.587	5.598	5.604	5.518	5.599	5.458	5.605
	HVSm	5.631	5.644	5.644	5.643	5.652	5.561	5.631	5.646	5.652	5.564	5.645	5.503	5.652
Img 3	PSNR	10.117	10.067	10.077	10.055	10.077	10.004	10.112	10.078	10.076	10.004	10.110	10.068	10.117
	Cielab	33.369	35.039	34.325	34.902	34.012	33.481	30.059	34.297	34.013	33.494	33.688	33.736	30.059
	HVS	4.885	4.870	4.875	4.860	4.881	4.802	4.909	4.872	4.877	4.802	4.885	4.765	4.909
	HVSm	4.922	4.915	4.920	4.909	4.929	4.842	4.940	4.919	4.925	4.843	4.925	4.804	4.940
Img 4	PSNR	10.024	10.131	10.130	10.126	10.149	10.018	10.015	10.142	10.155	10.020	10.120	10.057	10.155
	Cielab	23.499	24.042	24.037	23.940	23.797	23.475	21.925	24.145	23.797	23.478	23.770	23.531	21.925
	HVS	5.401	5.475	5.476	5.475	5.507	5.351	5.340	5.490	5.512	5.356	5.466	5.302	5.510

	HV Sm	5.524	5.583	5.585	5.584	5.617	5.460	5.455	5.608	5.620	5.462	5.577	5.412	5.620
Img 5	PSNR	10.190	10.157	10.157	10.153	10.164	10.093	10.194	10.158	10.164	10.094	10.079	10.119	10.194
	Cielab	24.323	24.678	24.686	24.697	24.572	24.473	23.179	24.699	24.574	24.484	24.528	24.824	23.179
	HV S	5.955	5.946	5.945	5.945	5.954	5.857	5.966	5.945	5.951	5.861	5.954	5.954	5.966
	HV Sm	5.989	5.988	5.998	5.987	5.997	5.896	5.997	5.989	5.995	5.901	5.993	5.994	5.997
Img 6	PSNR	10.143	10.098	10.182	10.060	10.090	10.055	10.185	10.166	10.084	10.056	10.150	10.170	10.185
	Cielab	43.312	48.498	43.884	46.864	45.645	42.464	35.442	43.767	45.730	42.491	43.765	39.539	35.442
	HV S	5.739	5.719	5.790	5.700	5.743	5.681	5.818	5.786	5.734	5.680	5.747	5.787	5.818
	HV Sm	5.802	5.790	5.861	5.778	5.826	5.745	5.868	5.859	5.818	5.743	5.811	5.846	5.868
Img 7	PSNR	10.020	9.976	9.986	9.964	9.983	9.893	10.058	9.981	9.981	9.893	10.014	9.992	10.058
	Cielab	32.933	34.448	33.976	34.261	33.576	33.243	29.206	33.889	33.582	33.255	33.312	32.182	29.206
	HV S	5.666	5.649	5.659	5.643	5.657	5.555	5.728	5.649	5.652	5.556	5.667	5.691	5.728
	HV Sm	5.698	5.690	5.700	5.686	5.701	5.591	5.752	5.691	5.696	5.592	5.702	5.725	5.752
Img 8	PSNR	9.996	9.987	9.990	9.980	9.998	9.902	10.005	9.991	9.998	9.903	10.004	9.967	10.005
	Cielab	28.777	29.597	29.334	29.578	29.134	28.893	26.591	29.364	29.136	28.871	29.052	29.219	26.591
	HV S	5.000	5.009	5.010	5.007	5.023	4.911	5.009	5.011	5.021	4.913	5.013	4.877	5.023
	HV Sm	5.051	5.064	5.065	5.063	5.079	4.964	5.056	5.067	5.077	4.966	5.066	4.928	5.079
Img 9	PSNR	10.097	10.095	10.095	10.092	10.091	10.050	10.109	10.097	10.094	10.050	10.098	10.062	10.109
	Cielab	16.984	17.076	17.041	17.104	17.411	16.878	16.455	17.118	17.412	16.872	17.009	18.142	16.455
	HV S	5.578	5.581	5.582	5.580	5.588	5.541	5.586	5.585	5.589	5.540	5.582	5.327	5.589
	HV Sm	5.605	5.608	5.608	5.608	5.616	5.568	5.609	5.613	5.616	5.567	5.609	5.355	5.616
Img 10	PSNR	10.294	10.299	10.299	10.294	10.306	10.229	10.293	10.302	10.308	10.228	10.307	10.245	10.308
	Cielab	26.000	26.431	26.381	26.435	26.248	25.978	24.679	26.448	26.249	26.024	26.189	26.315	24.679
	HV S	6.301	6.313	6.313	6.314	6.331	6.252	6.287	6.319	6.331	6.246	6.315	6.327	6.331
	HV Sm	6.362	6.374	6.373	6.374	6.391	6.312	6.344	6.379	6.391	6.306	6.374	6.389	6.391
Img 11	PSNR	10.442	10.441	10.414	10.404	10.417	10.336	10.448	10.413	10.417	10.336	10.438	10.384	10.448
	Cielab	28.611	29.431	29.209	29.441	29.023	28.787	26.537	29.257	29.024	28.775	28.815	29.563	26.537
	HV S	5.251	5.242	5.242	5.236	5.251	5.173	5.266	5.240	5.248	5.173	5.251	5.032	5.266
	HV Sm	5.285	5.283	5.283	5.279	5.293	5.211	5.296	5.281	5.290	5.211	5.288	5.067	5.296

Img 12	PSNR	10.142	10.134	10.137	10.126	10.146	10.062	10.140	10.139	10.147	10.062	10.150	10.125	10.150
	Cielab	29.851	30.864	30.646	30.799	30.307	29.791	27.068	30.645	30.311	29.801	30.204	29.612	27.068
	HVS	5.447	5.446	5.448	5.442	5.462	5.373	5.450	5.449	5.460	5.374	5.453	5.391	5.462
	HVSm	5.504	5.506	5.507	5.503	5.522	5.431	5.503	5.509	5.520	5.432	5.510	5.447	5.522
Average	PSNR	10.126	10.115	10.125	10.105	10.120	10.043	10.135	10.124	10.120	10.044	10.136	10.096	10.136
	Cielab	28.658	29.808	29.230	29.639	29.243	28.674	26.182	29.254	29.251	28.680	28.911	28.900	26.182
	HVS	5.414	5.417	5.424	5.412	5.430	5.340	5.426	5.425	5.427	5.341	5.424	5.317	5.430
	HVSm	5.463	5.469	5.476	5.466	5.484	5.390	5.470	5.478	5.481	5.391	5.474	5.365	5.484

For the results obtained from different denoising filters, instead of showing big tables like Table 1 above, we extracted the best performing results from those big tables and create summarized tables. Table 2 summarizes the best BM3D filtering results for three denoising configurations. It can be seen that the combination of GFPCA and post-denoising has the best performance. The PSNR value has been improved from 10 dB to 17.9 dB.

Table 3 summarizes the best wavelet denoising results for three denoising configurations. We can see that hybrid denoising has slight edge over the other configurations. The PSNR value has been improved from 10 dB to 17 dB. Table 4 summarizes the best diffusion denoising results for the three denoising configurations. It can be seen that the results are worse than other denoising algorithms. Table 5 to Table 7 summarize the median filtering results. We can observe that the 7x7 option achieved the best among the three median filters. Actually, the best performing method is the hybrid denoising using 7x7 median filter with GFPCA and the PSNR value has reached 22 dB from 10 dB. This is quite remarkable. Table 8 summarizes the FFDNET results. The performance is better than BM3D, wavelet, and diffusion, but worse than those median filters.

We also include some denoised images for the pre-denoising case in Figure 7. The post-denoising and hybrid denoising results can be found in Fig. A1 and Fig. A2 of the Appendix. It can be seen that the median filter with 7x7 size has the closest intensity to the ground truth. BM3D, wavelet, and FFDNET all have smooth results, but somehow their images look darker than the ground truth.

Table 2. Best performing BM3D denoising results for 10 dB noisy images. Bold numbers indicate the best in each row.

Metrics	Hybrid Denoising/ Best Algorithm	Post-Denoising / Best Algorithm	Pre-Denoising / Best Algorithm
PSNR (dB)	17.565/GFPCA	**17.901/GFPCA**	15.768/GFPCA
CIELAB	10.414/GFPCA	**10.209/GFPCA**	12.975/GFPCA
HVS (dB)	12.847/GFPCA	**13.228/GFPCA**	11.058/GFPCA
HVSm (dB)	13.038/GFPCA	**13.436/GFPCA**	11.203/GFPCA

Table 3. Best performing wavelet denoising results for 10 dB noisy images. Bold numbers indicate the best in each row.

Metrics	Hybrid Denoising/ Best Algorithm	Post-Denoising / Best Algorithm	Pre-Denoising / Best Algorithm
PSNR (dB)	**17.012/Baseline**	15.331/Standard	16.612/GFPCA
CIELAB	11.997/GFPCA	**12.860/GFPCA**	11.887/GFPCA
HVS (dB)	**11.955/Baseline**	10.511/GFPCA	11.599/GFPCA
HVSm (dB)	**12.177/Baseline**	10.641/GFPCA	11.775/GFPCA

Table 4: Best performing diffusion filter denoising results for 10 dB noisy images. Bold numbers indicate the best in each row.

Metrics	Hybrid Denoising/ Best Algorithm	Post-Denoising / Best Algorithm	Pre-Denoising / Best Algorithm
PSNR (dB)	**16.393/Baseline**	15.353/Standard	14.822/GFPCA
CIELAB	13.374/GFPCA	13.353/GFPCA	**14.490/GFPCA**
HVS (dB)	**11.318/Baseline**	10.466/Standard	9.851/GFPCA
HVSm (dB)	**11.524/Baseline**	10.652/Standard	9.969/GFPCA

Table 5. Best performing median filter (3x3) denoising results for 10 dB noisy images. Bold numbers indicate the best in each row.

Metrics	Hybrid Denoising/ Best Algorithm	Post-Denoising / Best Algorithm	Pre-Denoising / Best Algorithm
PSNR (dB)	19.362/GFPCA	**19.467/GFPCA**	18.841/GFPCA
CIELAB	8.905/GFPCA	**8.475/GFPCA**	9.438/GFPCA
HVS (dB)	14.444/GFPCA	**14.804/GFPCA**	13.963/GFPCA
HVSm (dB)	14.777/GFPCA	**15.138/GFPCA**	14.288/ GFPCA

Table 6. Best performing median filter (5x5) denoising results for 10 dB noisy images. Bold numbers indicate the best in each row.

Metrics	Hybrid Denoising/ Best Algorithm	Post-Denoising / Best Algorithm	Pre-Denoising / Best Algorithm
PSNR (dB)	**21.647/GFPCA**	21.218/GFPCA	21.405/GFPCA
CIELAB	**7.312/GFPCA`**	7.376/GFPCA	7.550/GFPCA
HVS (dB)	**16.791/GFPCA**	16.531/GFPCA	16.632/GFPCA
HVSm (dB)	**17.399/GFPCA**	17.069/GFPCA	17.266/GFPCA

Table 7. Best performing median filter (7x7) denoising results for 10 dB noisy images. Bold numbers indicate the best in each row.

Metrics	Hybrid Denoising/ Best Algorithm	Post-Denoising / Best Algorithm	Pre-Denoising / Best Algorithm
PSNR (dB)	**22.102/GFPCA**	21.552/GFPCA	21.927/GFPCA
CIELAB	**7.035/GFPCA**	7.140/GFPCA	7.257/GFPCA
HVS (dB)	**17.194/GFPCA**	16.708/GFPCA	17.073/GFPCA
HVSm (dB)	**17.857/GFPCA**	17.295/GFPCA	17.757/GFPCA

Table 8. Best performing FFDNET denoising results for 10 dB noisy images. Bold numbers indicate the best in each row.

Metrics	Hybrid Denoising/ Best Algorithm	Post-Denoising / Best Algorithm	Pre-Denoising / Best Algorithm
PSNR (dB)	17.761/GFPCA	**18.131/GFPCA**	17.020/HPM
CIELAB	10.686/GFPCA	**9.896/GFPCA**	11.655/GFPCA
HVS (dB)	13.123/GFPCA	**13.572/GFPCA**	12.309/HPM
HVSm (dB)	13.342/GFPCA	**13.797/GFPCA**	12.506/HPM

GT

Noisy Input

No Denoising/PRACS

BM3D/GFPCA

Wavelet/GFPCA

Diffusion/GFPCA

Medfilt 3x3/GFPCA

Medfilt 5x5/GFPCA
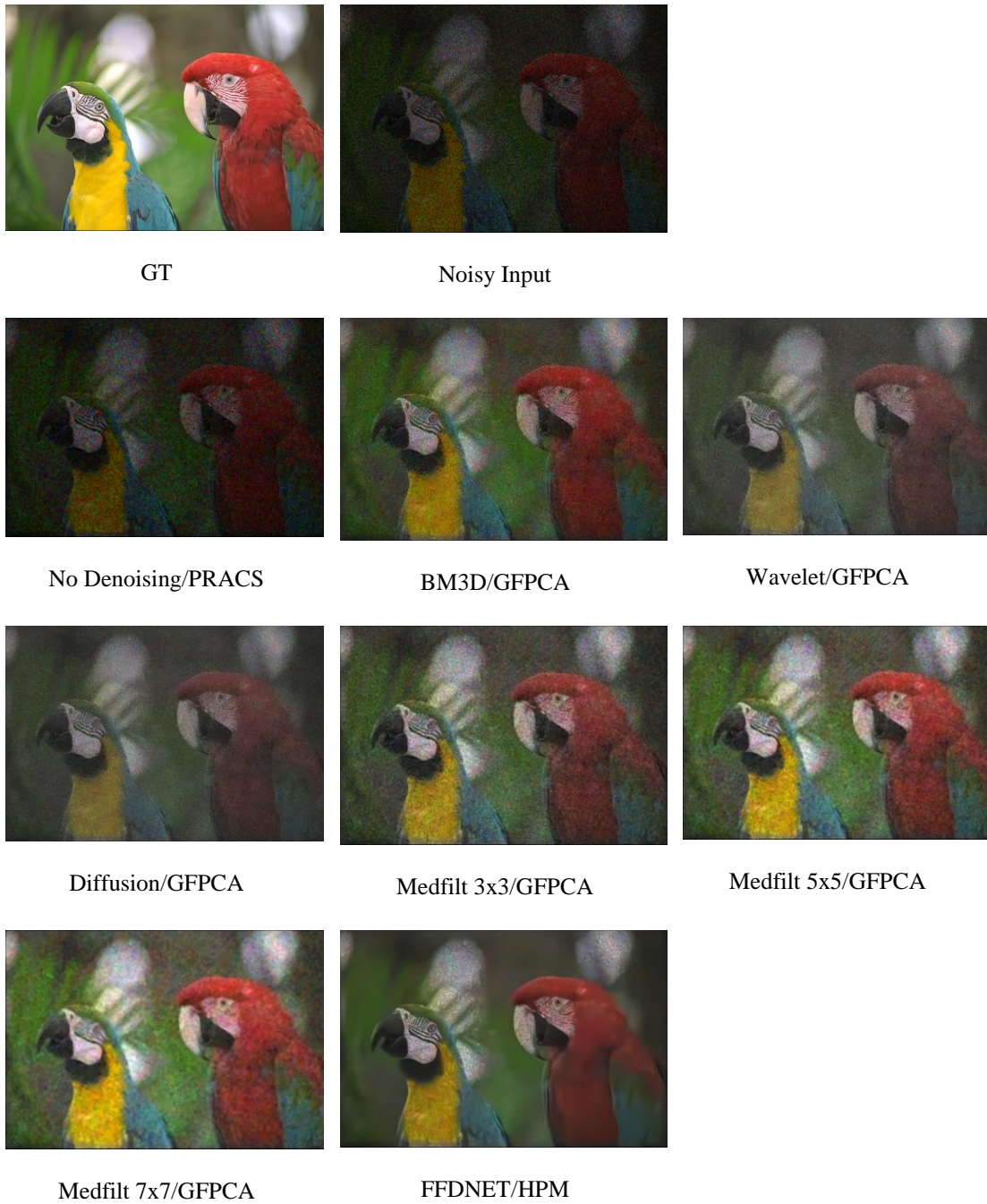

Medfilt 7x7/GFPCA

FFDNET/HPM

Figure 7. Demosaicing results using various pre-denoising approaches for 10 dB noisy images. For each image, a/b means the "a" is the denoising method and "b" is the pansharpening method.

3.2. 20 dB Noisy Images

We first present the demosaicing results without denoising in Table 9. This will help the comparison among those denoising results later. We observe that the averaged metrics in PSNR of all methods are all less than 20 dB, meaning that demosaicing alone cannot enhance the image quality.

Table 9. Demosaicing results without denoising for 20 dB Poisson noisy images.

Image		Baseline	Standard	GSA	HCM	SFIM	PCA	GFPCA	GLP	HPM	GS	PRACS	LSLCD	Best Score
Img1	PSNR	19.977	20.037	20.038	20.011	19.934	19.933	19.856	20.023	19.943	19.932	20.050	19.557	20.050
	Cielab	7.721	7.767	7.771	7.841	8.106	7.713	7.976	7.854	8.108	7.745	7.706	9.384	7.706
	HVS	14.529	14.558	14.558	14.541	14.547	14.384	14.376	14.557	14.548	14.470	14.562	13.590	14.562
	HVSm	14.620	14.638	14.638	14.627	14.635	14.461	14.457	14.643	14.637	14.549	14.641	13.669	14.643
Img2	PSNR	18.519	18.973	18.967	18.954	18.948	18.791	18.750	18.955	18.962	18.814	18.925	19.088	19.088
	Cielab	7.730	7.595	7.603	7.685	7.649	7.542	7.074	7.650	7.648	7.520	7.631	7.434	7.074
	HVS	14.106	14.363	14.377	14.368	14.393	14.185	14.109	14.385	14.392	14.196	14.355	14.114	14.393
	HVSm	14.334	14.505	14.513	14.506	14.531	14.317	14.298	14.527	14.533	14.332	14.503	14.232	14.533
Img3	PSNR	20.181	20.301	20.302	20.271	20.310	20.165	20.183	20.327	20.324	20.167	20.297	20.105	20.327
	Cielab	7.956	7.968	7.896	8.119	8.083	7.849	7.779	7.980	8.084	7.854	7.933	8.441	7.779
	HVS	15.101	15.176	15.177	15.175	15.212	15.041	15.045	15.211	15.216	15.050	15.173	14.713	15.216
	HVSm	15.245	15.292	15.292	15.290	15.324	15.158	15.164	15.324	15.328	15.168	15.292	14.824	15.328
Img4	PSNR	18.011	19.443	19.438	19.420	19.420	18.993	18.654	19.402	19.451	19.003	19.312	19.498	19.498
	Cielab	8.009	7.417	7.440	7.429	7.413	7.284	6.832	7.608	7.416	7.282	7.421	7.394	6.832
	HVS	14.118	14.942	14.952	14.957	15.050	14.468	14.090	15.016	15.054	14.467	14.866	14.770	15.054
	HVSm	14.726	15.290	15.296	15.299	15.416	14.823	14.551	15.379	15.423	14.825	15.252	15.081	15.423
Img5	PSNR	20.048	20.211	20.209	20.196	20.200	20.052	20.151	20.204	20.208	20.068	20.212	20.031	20.212
	Cielab	6.604	6.585	6.566	6.593	6.591	6.571	6.348	6.606	6.592	6.567	6.569	6.802	6.348
	HVS	15.873	16.000	16.001	15.997	16.019	15.787	15.866	16.016	16.018	15.824	15.996	15.892	16.019
	HVSm	16.044	16.126	16.127	16.123	16.144	15.911	15.998	16.145	16.146	15.951	16.126	16.027	16.146
Img6	PSNR	20.041	20.433	20.431	20.402	20.423	20.237	20.228	20.433	20.437	20.240	20.393	20.362	20.437
	Cielab	8.710	8.668	8.620	8.756	8.645	8.369	7.628	8.744	8.653	8.385	8.629	8.495	7.628
	HVS	15.852	16.095	16.080	16.105	16.153	15.946	15.785	16.121	16.157	15.919	16.046	15.884	16.157
	HVSm	16.159	16.321	16.311	16.325	16.377	16.181	16.030	16.352	16.382	16.151	16.293	16.091	16.382
Img7	PSNR	19.969	20.154	20.154	20.141	20.136	20.002	20.098	20.139	20.144	20.010	20.152	20.110	20.154
	Cielab	7.741	7.691	7.693	7.752	7.717	7.677	6.996	7.724	7.716	7.666	7.705	7.341	6.996
	HVS	15.752	15.874	15.875	15.875	15.880	15.711	15.805	15.866	15.878	15.720	15.870	15.852	15.880
	HVSm	15.908	15.997	15.997	15.996	16.006	15.829	15.938	15.994	16.005	15.839	15.994	15.968	16.006
Img8	PSNR	19.518	20.122	20.120	20.090	20.103	19.849	19.767	20.107	20.110	19.865	20.039	20.090	20.122
	Cielab	7.622	7.473	7.419	7.580	7.468	7.370	6.919	7.500	7.472	7.361	7.507	7.316	6.919
	HVS	14.901	15.295	15.310	15.317	15.357	15.015	14.918	15.334	15.349	15.032	15.257	14.869	15.357
	HVSm	15.181	15.473	15.483	15.486	15.531	15.189	15.142	15.514	15.527	15.210	15.453	15.030	15.531
Img9	PSNR	15.927	15.998	15.998	15.991	15.982	15.919	15.981	16.003	15.986	15.917	15.995	15.951	16.003
	Cielab	8.286	8.227	8.187	8.254	8.587	8.100	7.971	8.262	8.607	8.095	8.190	8.484	7.971
	HVS	11.458	11.503	11.502	11.502	11.519	11.431	11.469	11.516	11.522	11.428	11.498	11.284	11.522
	HVSm	11.529	11.555	11.555	11.554	11.571	11.483	11.522	11.567	11.573	11.480	11.553	11.336	11.573
Img10	PSNR	19.541	20.006	20.004	19.985	20.003	19.793	19.801	20.006	20.017	19.789	19.949	19.968	20.017
	Cielab	7.567	7.421	7.415	7.477	7.406	7.333	6.861	7.519	7.427	7.351	7.427	7.331	6.861
	HVS	15.738	16.043	16.024	16.057	16.110	15.856	15.737	16.075	16.114	15.822	15.982	16.037	16.114
	HVSm	16.060	16.248	16.238	16.253	16.309	16.078	15.984	16.283	16.314	16.042	16.217	16.233	16.314
Img11	PSNR	19.862	20.142	20.141	20.111	20.121	19.983	19.959	20.134	20.132	19.981	20.115	20.019	20.142
	Cielab	7.759	7.710	7.703	7.815	7.765	7.660	7.476	7.760	7.762	7.656	7.675	8.033	7.476
	HVS	14.955	15.074	15.075	15.070	15.093	14.940	14.875	15.086	15.093	14.936	15.064	14.610	15.093
	HVSm	15.126	15.203	15.203	15.200	15.223	15.068	15.021	15.217	15.224	15.064	15.199	14.730	15.224
Img12	PSNR	19.405	20.032	20.031	19.998	20.017	19.818	19.720	20.030	20.039	19.820	19.970	20.208	20.208
	Cielab	7.571	7.473	7.468	7.538	7.483	7.277	6.947	7.522	7.483	7.279	7.462	7.322	6.947
	HVS	15.389	15.636	15.636	15.638	15.675	15.426	15.380	15.660	15.681	15.429	15.620	15.471	15.681
	HVSm	15.704	15.844	15.844	15.843	15.887	15.634	15.617	15.873	15.894	15.637	15.840	15.639	15.894
Ave-rage	PSNR	19.250	19.654	19.653	19.631	19.633	19.461	19.429	19.647	19.646	19.467	19.618	19.582	19.654
	Cielab	7.773	7.666	7.649	7.737	7.743	7.562	7.234	7.727	7.746	7.563	7.655	7.815	7.234
	HVS	14.814	15.047	15.047	15.050	15.084	14.849	14.788	15.070	15.085	14.858	15.024	14.757	15.085
	HVSm	15.053	15.208	15.208	15.208	15.246	15.011	14.977	15.235	15.249	15.021	15.197	14.905	15.249

Table 10 summarizes the best BM3D filtering results for three denoising configurations. It can be seen that pre-denoising has the best performance. The PSNR value has been improved from 20 dB to 27.128 dB. Table 11 summarizes the best wavelet denoising results for three denoising configurations. We can see that hybrid denoising has slight edge over the other configurations. The PSNR value has been improved from 20 dB to 27 dB. Table 12 summarizes the best diffusion denoising results for the three denoising configurations. It can be seen that the results are worse than other denoising algorithms. Table 13 to Table 15 summarize the median filtering results. We can observe that the 3x3 option achieved the best among the three median filters. However, the median filter results are worse than BM3D and wavelet approaches. Table 16 summarizes the FFDNET results. The performance is better than BM3D, wavelet, and diffusion, but worse than those median filters.

We include some denoised images for the pre-denoising case in Figure 8. The post-denoising and hybrid denoising results can be found in Fig. A3 and Fig. A4 of the Appendix. It can be seen that the BM3D and medial filters have close resemblance to the ground truth. The wavelet and diffusion filter look dark as compared to the ground truth. Finally, FFDNET has over smoothed results.

Table 10. Best performing BM3D denoising results for 20 dB noisy images. Bold numbers indicate the best in each row.

Metrics	Hybrid Denoising/ Best Algorithm	Post-Denoising / Best Algorithm	Pre-Denoising / Best Algorithm
PSNR (dB)	27.122/Standard	24.963/GFPCA	**27.128/GSA**
CIELAB	3.845/Standard	4.326/GFPCA	**3.680/GFPCA**
HVS (dB)	**23.002/Standard**	20.623/GFPCA	23.071/SFIM
HVSm (dB)	23.895/Standard	21.394GFPCA	**23.992/SFIM**

Table 11. Best performing wavelet denoising results for 20 dB noisy images. Bold numbers indicate the best in each row.

Metrics	Hybrid Denoising/ Best Algorithm	Post-Denoising / Best Algorithm	Pre-Denoising / Best Algorithm
PSNR (dB)	**26.830/Standard**	23.364/GFPCA	**26.830/Standard**
CIELAB	4.793/GFPCA	4.936/GFPCA	**4.722/GFPCA**
HVS (dB)	**22.581/GSA**	18.783/GFPCA	22.559/SFIM
HVSm (dB)	**23.477/SFIM**	21.394/GFPCA	23.469/SFIM

Table 12. Best performing diffusion filter denoising results for 20 dB noisy images. Bold numbers indicate the best in each row.

Metrics	Hybrid Denoising/ Best Algorithm	Post-Denoising / Best Algorithm	Pre-Denoising / Best Algorithm
PSNR (dB)	**25.519/GSA**	23.178/GFPCA	25.367/Standard
CIELAB	5.415/GFPCA	**5.016/GFPCA**	5.242/GFPCA
HVS (dB)	**20.887/GSA**	18.614/GFPCA	20.702/GSA
HVSm (dB)	**21.511/GSA**	19.047/GFPCA	21.298/GSA

Table 13. Best performing median filter (3x3) denoising results for 20 dB noisy images. Bold numbers indicate the best in each row.

Metrics	Hybrid Denoising/ Best Algorithm	Post-Denoising / Best Algorithm	Pre-Denoising / Best Algorithm
PSNR (dB)	26.654/Standard	25.282/GFPCA	**26.661/GSA**
CIELAB	3.644/GFPCA	3.929/GFPCA	**3.580/GFPCA**
HVS (dB)	23.094/HCM	21.221/GFPCA	**23.169/Standard**
HVSm (dB)	24.419/Standard	22.219/GFPCA	**24.505/SFIM**

Table 14. Best performing median filter (5x5) denoising results for 20 dB noisy images. Bold numbers indicate the best in each row.

Metrics	Hybrid Denoising/ Best Algorithm	Post-Denoising / Best Algorithm	Pre-Denoising / Best Algorithm
PSNR (dB)	24.962/Standard	24.889/GFPCA	**25.001/GLP**
CIELAB	3.994/GFPCA	**3.886/GFPCA**	3.907/GFPCA
HVS (dB)	21.247/Standard	20.735/GFPCA	**21.377/SFIM**
HVSm (dB)	22.493/Standard	21.889/GFPCA	**22.648/SFIM**

Table 15. Best performing median filter (7x7) denoising results for 20 dB noisy images. Bold numbers indicate the best in each row.

Metrics	Hybrid Denoising/ Best Algorithm	Post-Denoising / Best Algorithm	Pre-Denoising / Best Algorithm
PSNR (dB)	23.710/Standard	24.346/Baseline	**23.768/GLP**
CIELAB	**4.453/GFPCA**	4.057/GFPCA	4.344/GFPCA
HVS (dB)	19.445/Standard	**19.963/Baseline**	19.550/GLP
HVSm (dB)	20.438/Standard	**21.027/Baseline**	20.558/GLP

Table 16. Best performing FFDNET denoising results for 20 dB noisy images. Bold numbers indicate the best in each row.

Metrics	Hybrid Denoising/ Best Algorithm	Post-Denoising / Best Algorithm	Pre-Denoising / Best Algorithm
PSNR (dB)	26.674/Standard	24.686/GFPCA	**26.676/GSA**
CIELAB	3.916/Standard	4.533/GFPCA	**3.914/GSA**
HVS (dB)	22.854/Standard	20.444/GFPCA	**22.960/SFIM**
HVSm (dB)	23.994/Standard	21.161/GFPCA	**24.124/SFIM**

GT   Noisy Input

No Denoising/Standard   BM3D/GSA   Wavelet/Standard

Diffusion/Standard   Medfilt 3x3/GSA   Medfilt 5x5/GLP

Medfilt 7x7/GLP   FFDNET/GSA

Figure 8. Demosaicing results using various pre-denoising approaches for 20 dB noisy images. For each image, a/b means the "a" is the denoising method and "b" is the pansharpening method.
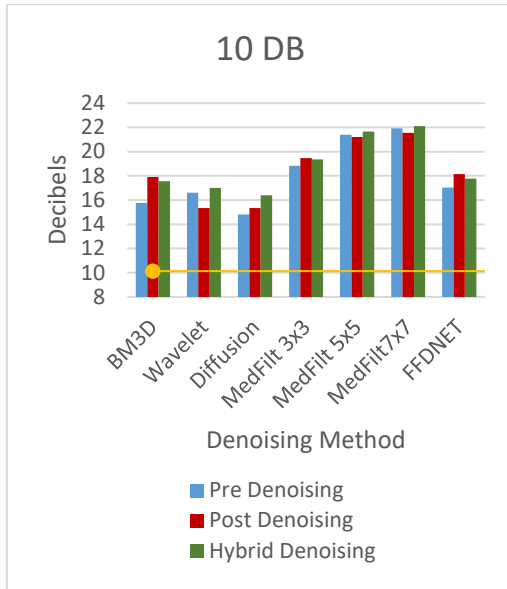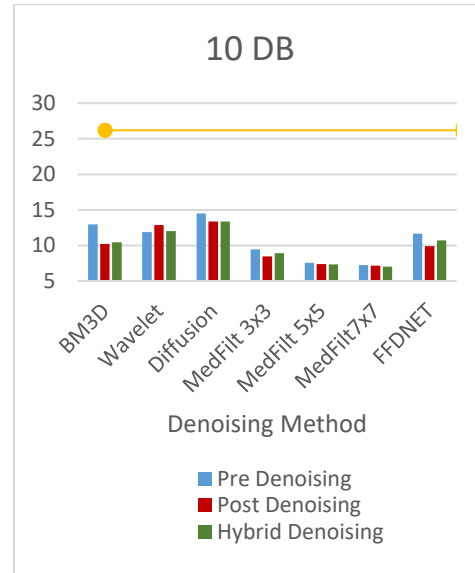
3.3. Discussions

3.3.1. 10 dB case

From the results in Sections 3.1 and 3.2, we have following observations:

- All filters improved over the no filtering case.
- Median filter with 7x7 has the best performance in all four metrics. It has improved the PSNR by more than 10 dBs.

- Median filter with 5x5 is the second best.
- The worst filter is the diffusion filter.
- Pre-filtering is better than post-filtering in wavelet, and median filters with 5x5 and 7x7 sizes. However, other filters have opposite behavior.
- FFDNET did not yield better performance than conventional filers.
- Hybrid did not yield additional gains over either pre-filtering or post-filtering.

(a) PSNR

(b) CIELAB
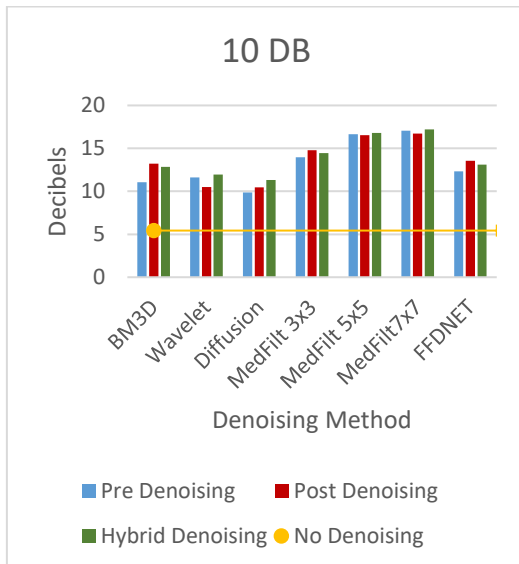
(c) HVS
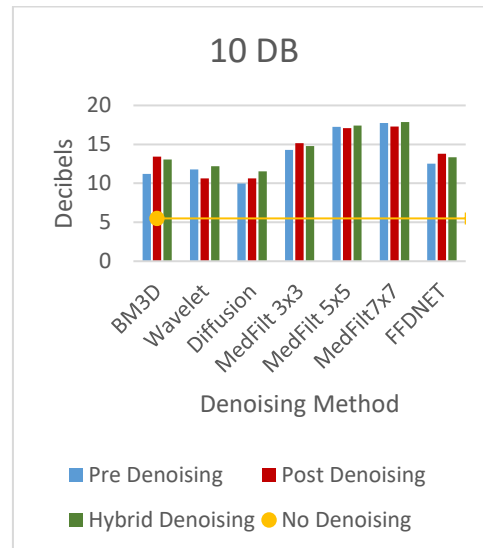
(d) HVSm

Figure 9. Comparison of different denoising methods for the 10 dB noisy images.

3.3.2.   20 dB case

For the 20 dB case, we have following observations:
•   All filters improved over the no filtering case.
•   BM3D filter has the best performance in all four metrics. It has improved the PSNR by more than 7 dBs.
•   Wavelet, median filter with 3x3, and FFDNET have close performance.
•   The worst filter is the median filter with 7x7. It appears that small filter size should be used for less noisy images.
•   Pre-filtering is better than post-filtering in all cases except the median filter with 7x7 size.
•   Hybrid did not yield any gains over either pre-filtering or post-filtering.

(a) PSNR

(b) CIELAB

(c) HVS

(d) HVSm
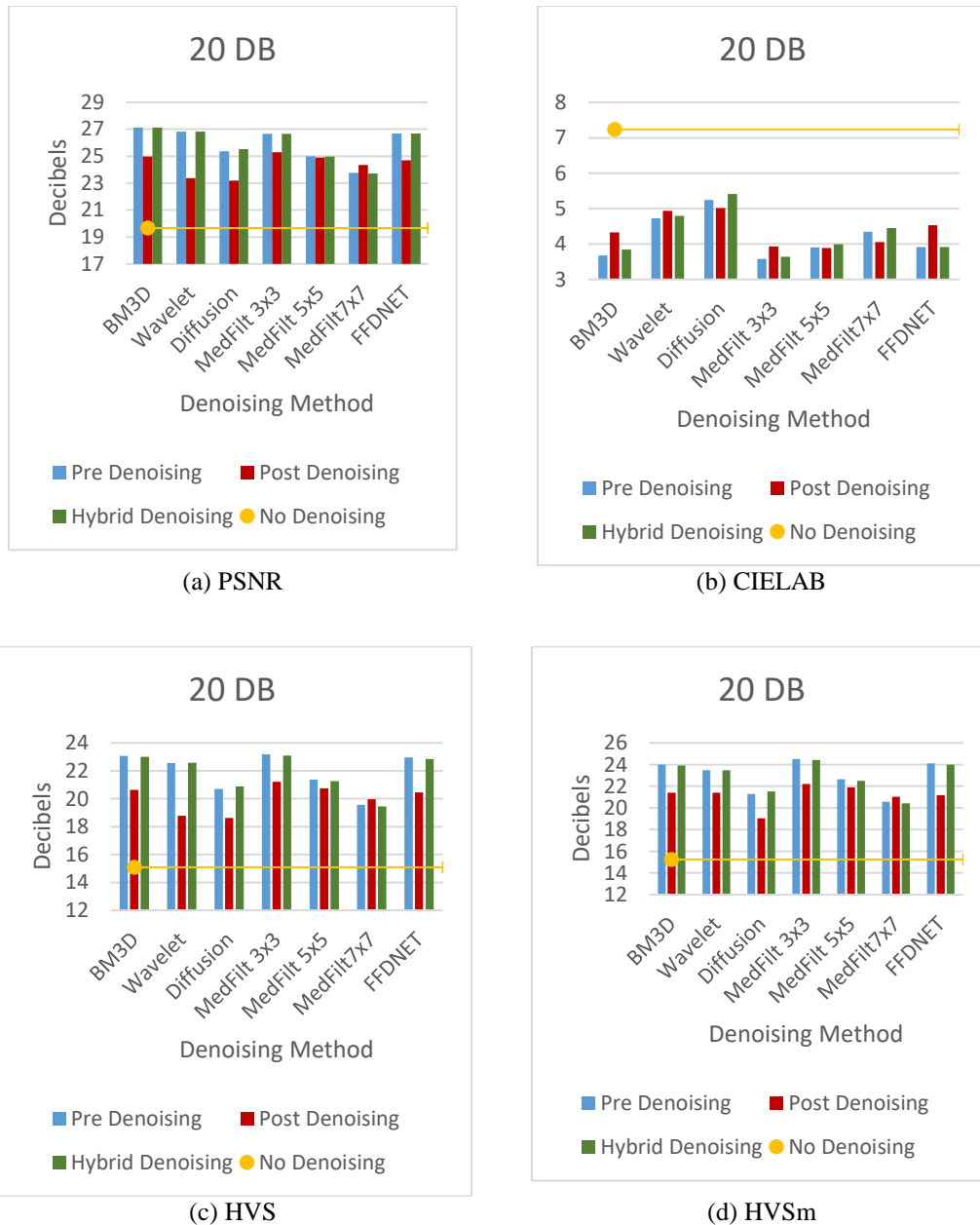
Figure 10. Comparison of different denoising methods for the 20 dB noisy images

4. CONCLUSIONS

Low light images have serious Poisson noise that affects the visual quality of images. In this paper, we present a thorough investigation of the various combination of denoising and demosaicing algorithms for low light images. Two noise levels (10 dB and 20 dB) were investigated using six conventional and one deep learning denoising algorithms. It was observed that, in serious low lighting conditions (10 dB), a conventional median filter can yield better performance than more advanced algorithms whereas in mild lighting conditions (20 dB), some modern algorithms such as BM3D and FFDNet start to have better results. One potential future direction is to look for some better deep learning based algorithms that can specifically deal with Poisson noise.

CONFLICT OF INTEREST

The authors declare no conflict of interest.

ACKNOWLEDGEMENTS

REFERENCES

[1]   B. E. Bayer, Color imaging array. US Patent 3,971,065, July 20, 1976.
[2]   J. F. Bell III, et al., "The Mars Science Laboratory Curiosity Rover Mast Camera (Mastcam) Instruments: Pre-Flight and In-Flight Calibration, Validation, and Data Archiving," AGU Journal Earth and Space Science, 2017.
[3]   M. Dao, C. Kwan, B. Ayhan, and J. F. Bell III, "Enhancing Mastcam Images for Mars Rover Mission," 14th International Symposium on Neural Networks, pp. 197-206, 2017.
[4]   C. Kwan, B. Budavari, M. Dao, B. Ayhan, J. F. Bell III, "Pansharpening of Mastcam images," IEEE International Geoscience and Remote Sensing Symposium, pp. 5117-5120, 2017.
[5]   B. Ayhan, M. Dao, C. Kwan, H. Chen, J. F. Bell III, and R. Kidd, "A Novel Utilization of Image Registration Techniques to Process Mastcam Images in Mars Rover with Applications to Image Fusion, Pixel Clustering, and Anomaly Detection," IEEE Journal of Selected Topics in Applied Earth Observations and Remote Sensing, 10(10), pp. 4553-4564, 2017.
[6]   J. Hamilton and J. Compton, Processing color and panchromatic pixels. U.S. Patent 20070024879A1, 2007.
[7]   T. Kijima, H. Nakamura, J. T. Compton, J. F. Hamilton, and T. E. DeWeese, Image sensor with improved light sensitivity. U.S. Patent 0 268 533, Nov., 2007.
[8]   C. Kwan and J. Larkin, "Demosaicing of Bayer and CFA 2.0 Patterns for Low Lighting Images," Electronics, 8, 1444, 2019.
[9]   M. Gharbi, G. Chaurasia, S. Paris, and F. Durand, "Deep joint demosaicking and denoising," ACM Trans. Graph, 35, 2016.
[10] C. Kwan, J. Larkin, and B. Ayhan, "Demosaicing of CFA 3.0 with Application to Low Lighting Images," Sensors, 20 (12), 3423, June 22, 2020.
[11] C. Kwan, J. Larkin, and B. Budavari, "Demosaicing of Real Low Lighting Images Using CFA 3.0," Signal & Image Processing: An International Journal (SIPIJ), vol. 11, no. 4, August 2020.
[12] C. Kwan and J. Larkin, "Demosaicing Mastcam Images Using A New Color Filter Array," Signal & Image Processing: An International Journal, 11 (3), 2020.
[13] L. Zhang, X. Wu, A. Buades, and X. Li, "Color demosaicking by local directional interpolation and nonlocal adaptive thresholding," J. Electron. Imaging, 20, 2011.
[14] BM3D denoising: http://www.cs.tut.fi/~foi/invansc/, accessed September 22, 2020.

[15] http://cs.haifa.ac.il/hagit/courses/seminars/wavelets/Presentations/Lecture09_Denoising.pdf, accessed September 22, 2020.

[16] P. Perona and J. Malik, "Scale-space and edge detection using anisotropic diffusion," Proceedings of IEEE Computer Society Workshop on Computer Vision. pp. 16–22, November 1987.

[17] https://www.mathworks.com/help/images/ref/imdiffusefilt.html, accessed September 22, 2020.

[18] R. C. Gonzalez and R. E. Woods, Digital Image Processing, 4th Edition, 2018 Pearson, 330 Hudson Street, New York, NY 10013.

[19] K. Zhang, W. Zuo, and L. Zhang, "FFDNet: Toward a Fast and Flexible Solution for CNN based Image Denoising. arXiv:1710.04026 [cs.CV], 22 May 2018.

[20] C. Kwan, B. Chou, L. M. Kwan, and B. Budavari, "Debayering RGBW Color Filter Arrays: A Pansharpening Approach," IEEE Ubiquitous Computing, Electronics & Mobile Communication Conference, pp. 94-100, New York City, 2017.

[21] G. Vivone, et al., "A Critical Comparison Among Pansharpening Algorithms," IEEE Trans. Geoscience and Remote Sensing, 53(5), 2015.

[22] J. G. Liu, "Smoothing filter based intensity modulation: A spectral preserve image fusion technique for improving spatial details," Int. J. Remote Sens., 21, 18, 2000.

[23] B. Aiazzi, et al., "MTF-tailored multiscale fusion of high-resolution MS and pan imagery," Photogramm. Eng. Remote Sens., 72(5), pp. 591–596, 2006.

[24] G. Vivone, et al., "Contrast and error-based fusion schemes for multispectral image pansharpening," IEEE Geosci. Remote Sensing Lett., 11(5), pp. 930–934, 2014.

[25] C. Laben and B. Brower, Process for enhancing the spatial resolution of multispectral imagery using pan-sharpening. U.S. Patent 6 011 875, Jan. 4, 2000.

[26] B. Aiazzi, et al., "Improving component substitution pansharpening through multivariate regression of MS+pan data," IEEE Trans. Geosci. Remote Sensing, 45(10), pp. 3230–3239, 2007.

[27] W. Liao, et al., "Processing of multiresolution thermal hyperspectral and digital color data: Outcome of the 2014 IEEE GRSS data fusion contest," IEEE J. Select. Top. Appl. Earth Observ. Remote Sensing, 8, 6, 2015.

[28] J. Choi, et al., "A new adaptive component-substitution based satellite image fusion by using partial replacement," IEEE Trans. Geosci. Remote Sens., 49, 1, 2011.

[29] J. Zhou, C. Kwan, and B. Budavari, "Hyperspectral image super-resolution: A hybrid color mapping approach," Journal of Applied Remote Sensing, 10, 3, article 035024, 2016.

[30] C. Kwan, J. H. Choi, S. Chan, J. Zhou, and B. Budavai, "Resolution Enhancement for Hyperspectral Images: A Super-Resolution and Fusion Approach," IEEE International Conference on Acoustics, Speech, and Signal Processing, pp. 6180 – 6184, New Orleans, 2017.

[31] C. Kwan, B. Budavari, and F. Gao, "A Hybrid Color Mapping Approach to Fusing MODIS and Landsat Images for Forward Prediction," Remote Sensing, 10 (4), 520, 2017.

[32] C. Kwan, B. Budavari, A. Bovik, and G. Marchisio, "Blind Quality Assessment of Fused WorldView-3 Images by Using the Combinations of Pansharpening and Hypersharpening Paradigms," IEEE Geoscience and Remote Sensing Letters, 14 (10), 1835-1839, 2017.

[33] C. Kwan, B. Ayhan, and B. Budavari, "Fusion of THEMIS and TES for Accurate Mars Surface Characterization," IEEE International Geoscience and Remote Sensing Symposium, pp. 3381-3384, 2017.

[34] L. Zhang and X. Wu, "Color demosaicking via directional linear minimum mean square-error estimation," IEEE Trans. Image Processing, 14, 2167–2178, 2005.

[35] W. Lu and Y. P. Tan, "Color filter array demosaicking: New method and performance measures," IEEE Trans. on Image Processing, 12, 1194–1210, 2003.

[36] E. Dubois, "Frequency-domain methods for demosaicking of Bayer-sampled color images," IEEE Signal Proc. Letters, 12, 847–850, 2005.

[37] B. Gunturk, Y. Altunbasak, and R. M. Mersereau, "Color plane interpolation using alternating projections," IEEE Trans. Image Processing, 11, 997–1013, 2002.

[38] X. Wu and N. Zhang, "Primary-consistent soft-decision color demosaicking for digital cameras," IEEE Trans. Image Processing, 13, 1263-1274, 2004.

[39] C. Kwan, X. Zhu, F. Gao, B. Chou, D. Perez, J. Li, Y. Shen, and K. Koperski, "Assessment of Spatiotemporal Fusion Algorithms for Planet and Worldview Images," Sensors, 18, 1051, 2018.

[40] K. Egiazarian, J. Astola, N. Ponomarenko, V. Lukin, F. Battisti, and M. Carli, "New full quality metrics based on HVS," In Proceedings of the Second International Workshop on Video Processing and Quality Metrics, Scottsdale, AZ, USA, 22–24 January 2006.

[41] N. Ponomarenko, F. Silvestri, K. Egiazarian, M. Carli, J. Astola, and V. Lukin, "On between-coefficient contrast masking of DCT basis functions," In Proceedings of the Third International Workshop on Video Processing and Quality Metrics for Consumer Electronics VPQM-07, Scottsdale, AZ, USA, 25–26 January 2007.

[42] X. Zhang and B. A. Wandell, "A spatial extension of cielab for digital color image reproduction," SID Journal, 1997.

[43] C. Kwan, J. Larkin, B. Budavari, B. Chou, E. Shang, and T. D. Tran, "A comparison of compression codecs for maritime and sonar images in bandwidth constrained applications," Computers, 8 (2), 32, April 28, 2019.

[44] C. Kwan, J. Larkin, B. Budavari, E. Shang, and T. Tran, "Perceptually Lossless Compression with Error Concealment for Periscope and Sonar Videos," Signal & Image Processing: An International Journal (SIPIJ), 10 (4), April 30, 2019.

Appendix

GT

Noisy Input

No Denoising/PRACS

BM3D/GFPCA

Wavelet/Standard

Diffusion/Standard

Medfilt 3x3/GFPCA

Medfilt 5x5/GFPCA

Medfilt 7x7/GFPCA

FFDNET/GFPCA

Fig. A1. Demosaicing results using various post-denoising approaches for 10 dB noisy images. For each image, a/b means the "a" is the denoising method and "b" is the pansharpening method.

GT

Noisy Input

No Denoising/PRACS

BM3D/GFPCA

Wavelet/Baseline

Diffusion/Baseline

Medfilt 3x3/GFPCA

Medfilt 5x5/GFPCA

Medfilt 7x7/GFPCA

FFDNET/GFPCA

Fig. A2. Demosaicing results using various hybrid-denoising approaches for 10 dB noisy images. For each image, a/b means the "a" is the denoising method and "b" is the pansharpening method.

GT

Noisy Input

No Denoising/Standard

BM3D/GFPCA

Wavelet/GFPCA

Diffusion/GFPCA

Medfilt 3x3/GFPCA

Medfilt 5x5/GFPCA
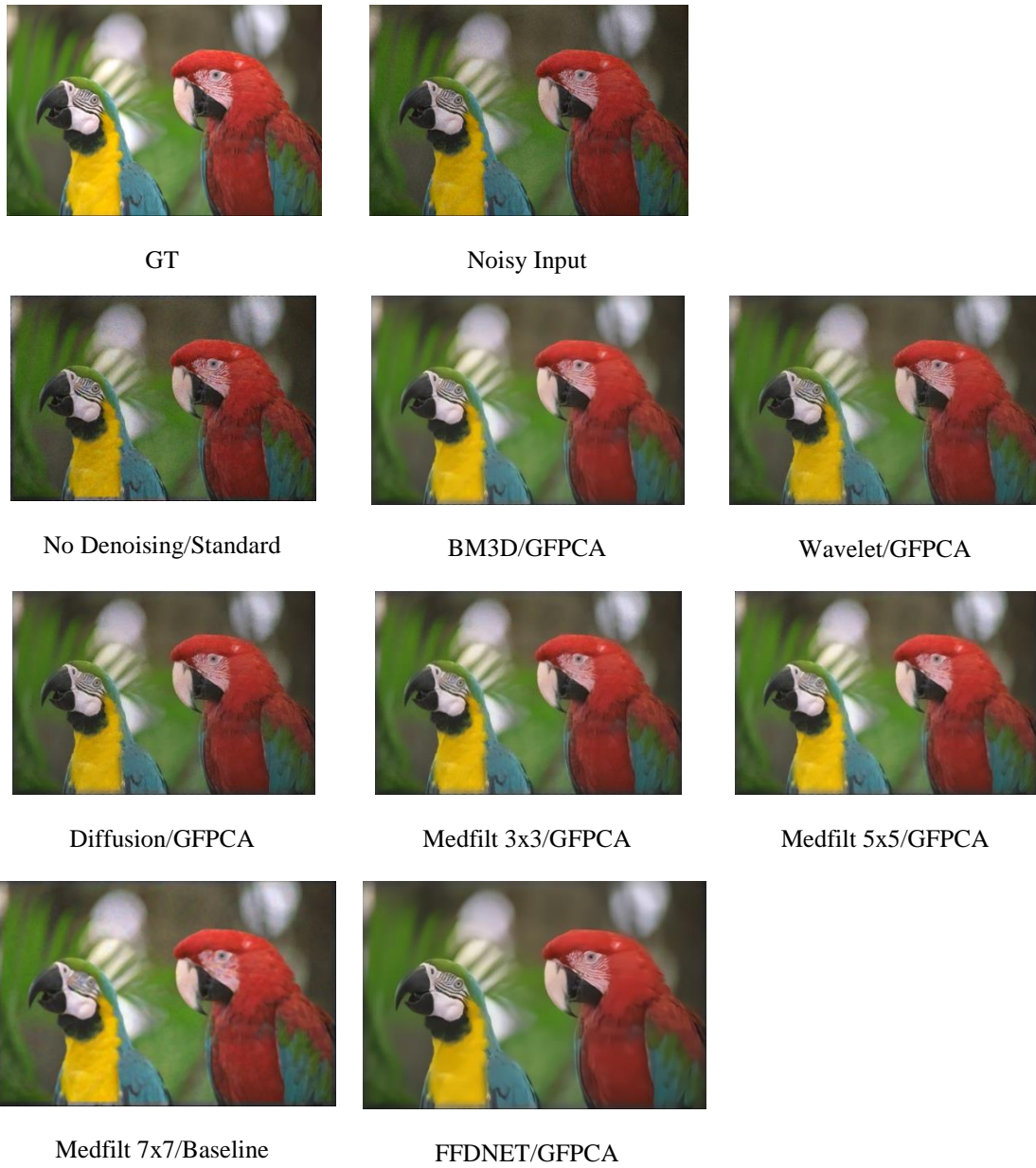
Medfilt 7x7/Baseline

FFDNET/GFPCA

Fig. A3. Demosaicing results using various post-denoising approaches for 20 dB noisy images. For each image, a/b means the "a" is the denoising method and "b" is the pansharpening method.

GT

Noisy Input

No Denoising/Standard

BM3D/Standard

Wavelet/Standard

Diffusion/GSA

Medfilt 3x3/Standard

Medfilt 5x5/Standard
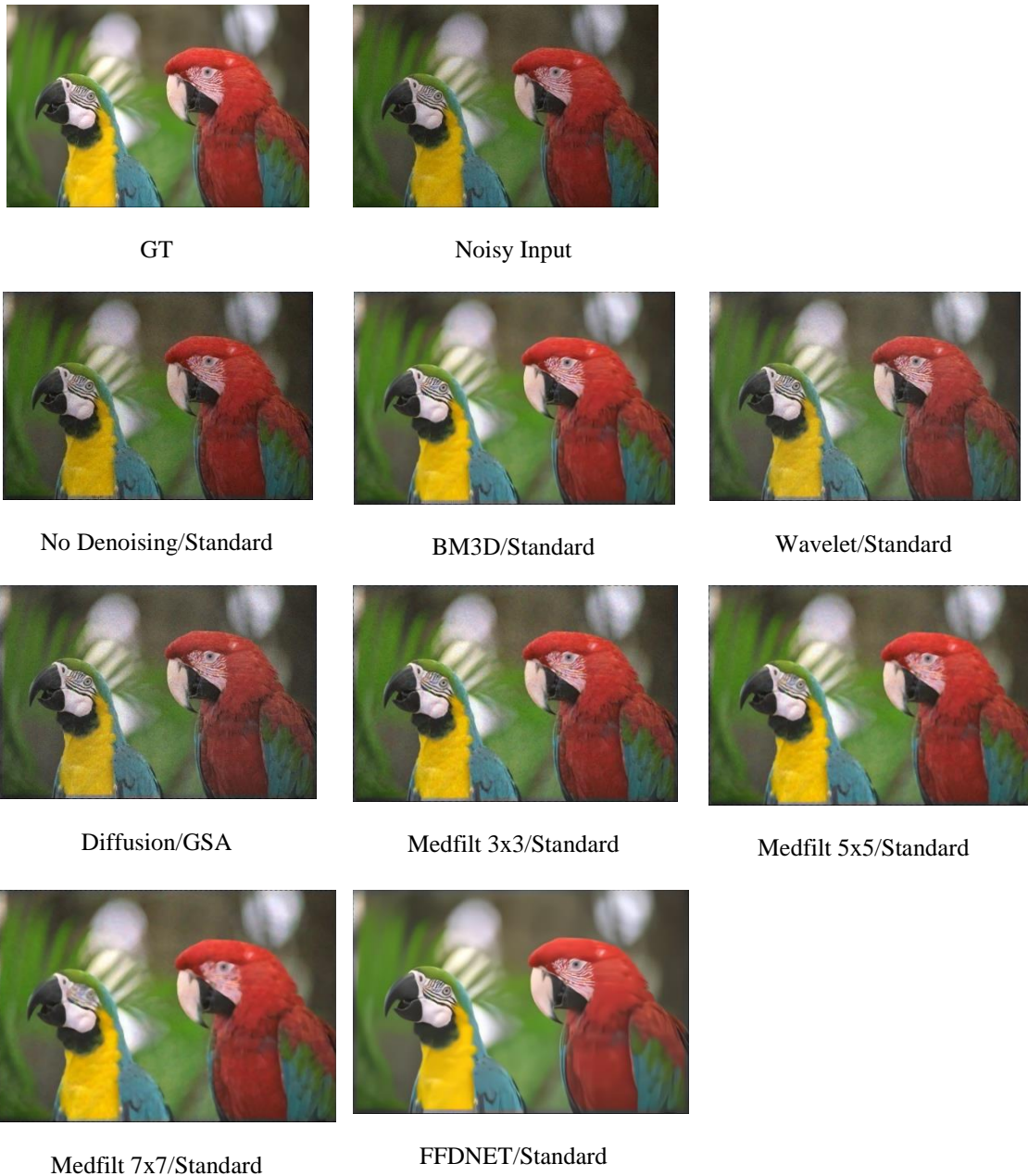
Medfilt 7x7/Standard

FFDNET/Standard

Fig. A4. Demosaicing results using various hybrid-denoising approaches for 20 dB noisy images. For each image, a/b means the "a" is the denoising method and "b" is the pansharpening method.

AUTHORS

Chiman Kwan received his Ph.D. degree in electrical engineering from the University of Texas at Arlington in 1993. He has one book, four book chapters, 15 patents, 65 invention disclosures, 375 technical papers in journals and conferences, and 550 technical reports. Over the past 25 years, he has been the PI/Program Manager of over 120 diverse projects with total funding exceeding 36 million dollars. He is also the founder and Chief Technology Officer of Signal Processing, Inc. and Applied Research LLC. He received numerous awards from IEEE, NASA, and some other agencies.

Jude Larkin received his B.S. in Computer Science from Franciscan University of Steubenville in 2015. He is a software engineer at ARLLC. He has been involved in diverse projects, including mission planning for UAVs, image fusion, image demosaicing, and remote sensing.